Available online at www.sciencedirect.com
ScienceDirect
Journal of Sound and Vibration 321 (2009) 363–374
JOURNAL OF SOUND AND VIBRATION
www.elsevier.com/locate/jsvi

A numerical model for calculating vibration due to a harmonic moving load on a floating-slab track with discontinuous slabs in an underground railway tunnel

M.F.M. Hussein[a,*], H.E.M. Hunt[b,1]

[a]School of Civil Engineering, University of Nottingham, University Park, Nottingham NG7 2RD, UK
[b]Engineering Department, Cambridge University, Trumpington Street, Cambridge CB2 1PZ, UK

Received 17 August 2007; received in revised form 8 September 2008; accepted 12 September 2008
Handling Editor: A.V. Metrikine
Available online 21 October 2008

Abstract

This paper presents a new method for modelling floating-slab tracks with discontinuous slabs in underground railway tunnels. The track is subjected to a harmonic load moving with a constant velocity. The model consists of two sub-models. The first is an infinite track with periodic double-beam unit formulated as a periodic infinite structure. The second is modelled with a new version of the Pipe-in-Pipe (PiP) model that accounts for a tunnel wall embedded in a half-space. The two sub-models are coupled by writing the force transmitted from the track to the tunnel as a continuous function using Fourier series representation and satisfying the compatibility condition.

The displacements at the free surface are calculated for a track with discontinuous slab and compared with those of a track with continuous slab. The results show that the far-field vibration can be significantly increased due to resonance frequencies of slabs for tracks with discontinuous slabs.

1. Introduction

Vibration generated by trains is a serious concern for inhabitants of buildings in close proximity to underground tunnels. Inhabitants perceive vibration either directly due to vibration of floors and walls or indirectly as re-radiated noise. Vibration can also cause disturbance due to movement of household objects, especially mirrors or due to rattling of windowpanes and glassware. The problem can be more serious in some circumstances such as where an underground tunnel is passing below sensitive buildings, e.g. a concert hall. The frequency range for vibration from underground railways is 0–200 Hz. Vibration at higher frequencies is generally attenuated rapidly with distance along the transmission path through the ground.

One of the effective means for reducing vibration from underground railways is the use of floating-slab tracks [1–3]. The track is isolated from the track bed via rubber bearings or steel springs. The slab can be cast

*Corresponding author. Tel.: +44 1159 513904; fax: +44 1159 513898.
E-mail addresses: mohammed.hussein@nottingham.ac.uk (M.F.M. Hussein), hemh1@cam.ac.uk (H.E.M. Hunt).
[1]Tel.: +44 1223 332730; fax: +44 1223 332662.

0022-460X/$ - see front matter © 2008 Elsevier Ltd. All rights reserved.
doi:10.1016/j.jsv.2008.09.023

in-situ leading to a track with a continuous slab. It may also be constructed in discrete pre-cast sections leading to a track with a discontinuous slab. Examples of floating-slab tracks are the 1.5 m slab in Toronto, the 3.4 m Eisenmann track in Munich and Frankfurt, the 7 m slab in New York subway and the WMATA continuous slab system in Washington, DC.

A number of models of floating-slab tracks with continuous slabs are presented in the literature for both surface and underground railway tracks. Shamalta and Metrikine [4] presented a model of an embedded railway track. The model uses a flexible plate to account for a slab track and an elastic foundation to account for the ground. This model can be used to account for floating-slab tracks by incorporating the stiffness of both slab bearings and the ground in the elastic foundation. Hussein and Hunt [5] present a model of floating-slab tracks with continuous slabs on elastic foundations. The slab is modelled as an Euler–Bernoulli beam.

There are other models of floating-slab tracks with continuous slabs which account more accurately for the track bed. These models are useful for the calculations of the far-field vibration. For surface railways, the track bed can be modelled as an elastic half-space [6]. For underground railways, a tunnel and its surrounding soil are incorporated in the model and the ground can be modelled as an elastic full-space or an elastic half-space [7–9].

Floating-slab tracks with discontinuous slabs on elastic foundations are modelled by Hussein and Hunt [10,11]. These tracks have more resonances compared to tracks with continuous slabs. These resonances occur at the natural frequencies of the discrete slab [10]. The model presented in Ref. [10] is useful in understanding the dynamic effect of slab discontinuity on vibration induced at the track bed. However, the tunnel and its surrounding soil should be considered to account for the track-tunnel-soil interaction and to provide the necessary transfer functions for the calculations of the far-field response due to a load applied on the track.

In this paper, a model of floating-slab track with discontinuous slab resting on a tunnel embedded in a half-space is presented. The model accounts for a harmonic load moving on the track with a constant velocity. The model can be used by engineers responsible of designing of vibration countermeasures in underground railway tunnels when considering floating-slab tracks with discontinuous slabs. In such a case, the model can be used to compute the slab motion with a view to design to prevent long-term degradation and consequent maintenance problems.

The model consists of two sub-models. The first is a periodically-inhomogeneous model to account for an infinite track with periodic double-beam units. The second is a homogeneous model to account for a tunnel embedded in a half-space [12]. The two sub-models are coupled by writing the force transmitted from the track to the tunnel as a continuous function using Fourier series representation and satisfying the compatibility condition.

The method presented in this paper contributes to the modelling techniques for periodically-inhomogeneous systems. The method tackles the problem of coupling a periodically-inhomogeneous system to a homogeneous system and therefore can be used for modelling of other problems falling under the same class. A number of methods are presented in the literature for modelling of periodically-inhomogeneous systems. These methods and some of their applications are reviewed in the next paragraphs.

Jezequel [13] uses the Fourier series approach to analyse an infinite beam supported periodically by lateral and torsion stiffness. The main characteristic of this approach is that a single differential equation is used to describe the behaviour of the beam with respect to time and space. To do this, a summation of a series of delta functions is used to account for discontinuities at periodic distances. Steady-state solutions are written as a summation of Fourier series with unknown coefficients. These solutions are substituted in the equations of motion and the results are Fourier transformed to give a set of algebraic equations. The coefficients are found by solving this set of equations. Jezequel only considers non-oscillating moving loads. Kisilowski et al. [14] present a mathematical solution based on the same method but including a moving wheel on a periodically supported rail. Ilias and Muller [15] use the same approach to analyse a discretely supported rail under a harmonic moving load and under a moving wheel-set.

Krzyzynski [16] uses the Floquet's method to model a harmonic moving load on an Euler–Bernoulli beam mounted on discrete infinite supports. This method takes advantage of periodicity in the longitudinal direction where Floquet's solution of the differential equation is used. Muller et al. [17] provide comparison between the Fourier series approach and Floquet's method. An undamped Euler–Bernoulli beam is compared with the corresponding Timoshenko beam with very high shear stiffness, very low rotational inertia and very low

damping. Nordborg [18] models an Euler–Bernoulli beam mounted on different kinds of discrete supports to calculate a closed-form solution of a track under non-moving oscillating loads. He transforms equations of motion to the wavenumber-frequency domain and these are solved using Floquet's theorem. In a second paper [19], he calculates the rail response for a moving oscillating load on the rail using results of Green's function in the frequency-space domain from Ref. [18]. To calculate the frequency domain response at a specific rail point, integration is performed in the space domain for Green's function multiplied by the frequency-domain force at a certain frequency.

Smith and Wormley [20] use the periodicity-condition method to model a moving constant load on an infinite Euler–Bernoulli beam supported periodically on rigid supports. In this method, calculations are made only for one repeating unit. Response of any other unit is calculated using the periodicity condition. Equations of motion of the unit under consideration are transformed to the frequency domain. The resulting differential equations are solved as a summation of homogenous and particular solutions. The homogenous solution coefficients are found by considering the boundary condition at the end of the unit under consideration. Belotserkovskiy [21] uses the same method to analyse a rail modelled as an Euler–Bernoulli beam on a Winkler foundation with resilient hinges to represent rail joints under a harmonic-moving load. He also uses this method to analyse a Timoshenko beam on discrete supports to account for sleepers. Metrikine and Bosch [22] use the periodicity-condition method to study the dynamic response of a system of two level catenary to a moving load. The catenary system consists of two infinite strings (upper and lower) connected by lumped mass-spring-dashpot elements which are positioned equidistantly along the strings. The upper string is fixed at periodically spaced fixation points.

This paper is organised in the following sections. Section 2 presents the model formulation. Section 3 presents results of the model where the response in the free-surface due to a harmonic load moving on the track with a constant velocity is shown and compared to those resulting from a track with a continuous slab. The main relationships of the periodic-structure theory are derived and presented in Appendix A to facilitate other derivations presented in Section 2 of the paper.

2. Formulation of the model

The model used in this paper is shown in Fig. 1. The two rails of the track are modelled as a single Euler–Bernoulli beam which is supported on a slab via continuous layer of springs to account for railpads. The slab is modelled as Euler–Bernoulli beam supported on the tunnel invert via another layer of springs to account for slab bearings. The tunnel and soil are formulated using a new version of the PiP (Pipe-in-Pipe) model [12]. This version accounts for a tunnel embedded in a half-space by using the elastic continuum theory for a tunnel in a full-space along with Green's functions for an elastic half-space.

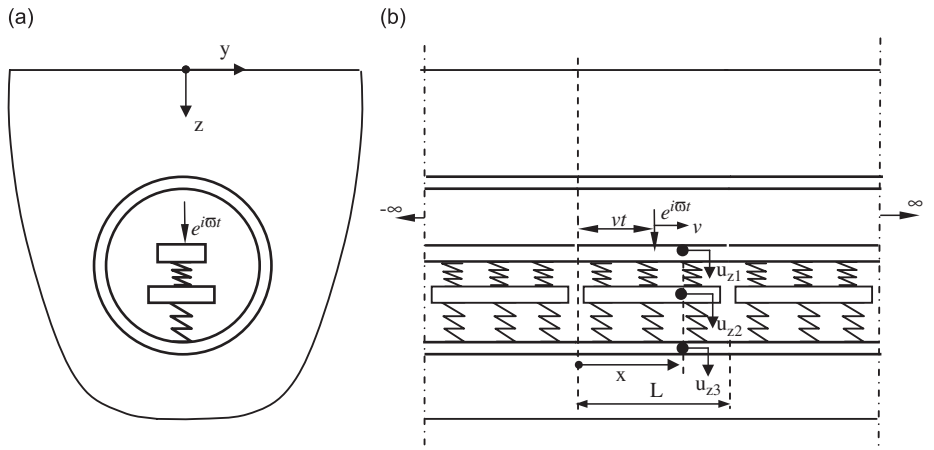

Fig. 1. A model of a floating-slab track with discontinuous slab of length L subjected to a harmonic load moving with a constant velocity along the track: (a) end view and (b) side view.

For the model shown in Fig. 1, the governing equations of the unit of the track in the range ($0 \leqslant x \leqslant L$), in the space-time domain can be written as

$$EI_1 \frac{\partial^4 u_{z1}}{\partial x^4} + m_1 \frac{\partial^2 u_{z2}}{\partial t^2} + k_1(u_{z1} - u_{z2}) = e^{i\varpi t}\delta(x - vt), \tag{1}$$

$$EI_2 \frac{\partial^4 u_{z2}}{\partial x^4} + m_2 \frac{\partial^2 u_{z2}}{\partial t^2} - k_1(u_{z1} - u_{z2}) + R = 0, \tag{2}$$

$$R = k_2(u_{z2} - u_{z3}), \tag{3}$$

with boundary conditions (see Eq. (26) for more details)

$$\frac{\partial^j u_{z1}(L,t)}{\partial x^j} = e^{i(\varpi L/v)} \frac{\partial^j u_{z1}(0,t)}{\partial x^j} \quad \text{for } j = 0,1,2,3, \tag{4}$$

$$\frac{\partial^j u_{z2}(L,t)}{\partial x^j} = \frac{\partial^j u_{z2}(0,t)}{\partial x^j} = 0 \quad \text{for } j = 2,3, \tag{5}$$

where u_{z1}, u_{z2} and u_{z3} are the displacement of the rails, the slab and the track bed, i.e. the tunnel, respectively. R is the slab-bearings' compressive force per unit length. This force is acting upwards at the bottom of the slab and downwards at the tunnel. EI_1 and EI_2 are the bending stiffness of the rails (for two rails) and the slab, respectively. m_1 and m_2 are the mass per unit length of the rails (for two rails) and the slab, respectively. k_1 and k_2 are the stiffness per unit length of the railpads (for two rails) and the slab bearings, respectively. ϖ is the excitation frequency and v is the velocity of the moving load.

Eqs. (1)–(5) are transformed to the space-frequency domain using Fourier transformation to give

$$EI_1 \frac{d^4 \tilde{u}_{z1}}{dx^4} - m_1\omega^2 \tilde{u}_{z1} + k_1(\tilde{u}_{z1} - \tilde{u}_{z2}) = \frac{1}{v} e^{i((\varpi-\omega)/v)x}, \tag{6}$$

$$EI_2 \frac{d^4 \tilde{u}_{z2}}{dx^4} - m_2\omega^2 \tilde{u}_{z2} - k_1(\tilde{u}_{z1} - \tilde{u}_{z2}) + \tilde{R} = 0, \tag{7}$$

$$\tilde{R} = k_2(\tilde{u}_{z2} - \tilde{u}_{z3}), \tag{8}$$

with boundary conditions

$$\frac{d^j \tilde{u}_{z1}(L,\omega)}{dx^j} = e^{i((\varpi-\omega)/v)L} \frac{d^j \tilde{u}_{z1}(0,\omega)}{dx^j} \quad \text{for } j = 0,1,2,3, \tag{9}$$

$$\frac{d^j \tilde{u}_{z2}(L,\omega)}{dx^j} = \frac{d^j \tilde{u}_{z2}(0,\omega)}{dx^j} = 0 \quad \text{for } j = 2,3. \tag{10}$$

As demonstrated in Appendix A, using the periodic-structure theory, the induced force at the tunnel invert can be written in the following form in the space-frequency domain (see Eq. (32) for more details)

$$\tilde{R}(x,\omega) = \sum_{n=-\infty}^{\infty} b_n(\omega) e^{i(\xi_n + (\varpi/v) - (\omega/v))x} \quad \text{with } \xi_n = 2\pi n/L. \tag{11}$$

The displacement at the tunnel invert can be calculated by transforming Eq. (11) to the wavenumber-frequency domain and multiply the result by the Frequency Response Function (FRF) at the tunnel invert to give

$$\tilde{u}_{z3}(\xi,\omega) = \tilde{H}_t(\xi,\omega) \sum_{n=-\infty}^{\infty} b_n(\omega) 2\pi\delta\left(\xi - \xi_n - \frac{\varpi}{v} + \frac{\omega}{v}\right), \tag{12}$$

where $\tilde{H}_t(\xi,\omega)$ is the FRF of the tunnel invert, i.e. the displacement of the tunnel due to a unit excitation on the tunnel in the wavenumber-frequency domain. Eq. (12) can now be transformed to the space-frequency

domain to give

$$\tilde{u}_{z3}(x,\omega)=\sum_{n=-\infty}^{\infty} b_n(\omega)\tilde{H}_t\Big(\xi_n+\frac{\varpi}{v}-\frac{\omega}{v},\omega\Big)\mathrm{e}^{\mathrm{i}(\xi_n+(\varpi/v)-(\omega/v))x}. \tag{13}$$

The displacement at any point in the soil can be calculated by replacing the FRF on the right-hand side of Eq. (13) by the transfer function between that point and the tunnel invert.

The purpose of the rest of analysis is to determine the coefficients $b_n(\omega)$ for given parameter values of the track and for a prescribed ϖ and v. Eqs. (6) and (7) can be written in the following form (using Eq. (11) to substitute for $\tilde{R}$)

$$\begin{bmatrix} EI_1 & 0 \\ 0 & EI_2 \end{bmatrix}\frac{\mathrm{d}^4\tilde{u}_z}{\mathrm{d}x^4}+\begin{bmatrix} k_1-m_1\omega^2 & -k_1 \\ -k_1 & k_1-m_2\omega^2 \end{bmatrix}\tilde{u}_z=\begin{bmatrix}1\\0\end{bmatrix}(1/v)\mathrm{e}^{\mathrm{i}((\varpi-\omega)/v)x}+\sum_{n=-\infty}^{n=\infty}\begin{bmatrix}0\\-1\end{bmatrix}b_n(\omega)\mathrm{e}^{\mathrm{i}(\xi_n+(\varpi/v)-(\omega/v))x}, \tag{14}$$

where $\tilde{u}_z(x,\omega)=[\tilde{u}_{z1}(x,\omega),\tilde{u}_{z2}(x,\omega)]^{\mathrm{T}}$. The solution of Eq. (14) is written as a superposition of the homogeneous solution and solutions resulting from each term of the right-hand side expression. The complete solution reads

$$\tilde{u}_z(x,\omega)=\sum_{p=1}^{8} a_p\tilde{Z}_p\mathrm{e}^{\mathrm{i}\phi_p x}+\tilde{U}\mathrm{e}^{\mathrm{i}((\varpi/v)-(\omega/v))x}+\sum_{n=-\infty}^{\infty}\tilde{V}_n b_n\mathrm{e}^{\mathrm{i}(\xi_n+(\varpi/v)-(\omega/v))x}, \tag{15}$$

where a_p are the coefficients of the homogeneous solution. ϕ_p and $\tilde{Z}_p$ are the eigenvalues and eigenvectors of the homogeneous solution. These are calculated from the following equation

$$\begin{bmatrix} EI_1\phi_p^4-m_1\omega^2+k_1 & -k_1 \\ -k_1 & EI_2\phi_p^4-m_2\omega^2+k_1 \end{bmatrix}\tilde{Z}_p=\begin{bmatrix}0\\0\end{bmatrix}. \tag{16}$$

$\tilde{U}$ is the vector of coefficients of the particular solutions for the first term in the expression in the right-hand side of Eq. (14). $\tilde{U}$ is calculated from the following equation

$$\tilde{U}=\begin{bmatrix} EI_1\Big(\dfrac{\varpi-\omega}{v}\Big)^4-m_1\omega^2+k_1 & -k_1 \\ -k_1 & EI_2\Big(\dfrac{\varpi-\omega}{v}\Big)^4-m_2\omega^2+k_1 \end{bmatrix}^{-1}\begin{bmatrix}1/v\\0\end{bmatrix}. \tag{17}$$

$\tilde{V}_n$ is the vector of coefficients of the particular solutions for the nth term of the summation on the right-hand side of Eq. (14). $\tilde{V}_n$ is calculated from the following equation

$$\tilde{V}_n=\begin{bmatrix} EI_1\Big(\xi_n+\dfrac{\varpi}{v}-\dfrac{\omega}{v}\Big)^4-m_1\omega^2+k_1 & -k_1 \\ -k_1 & EI_2\Big(\xi_n+\dfrac{\varpi}{v}-\dfrac{\omega}{v}\Big)^4-m_2\omega^2+k_1 \end{bmatrix}^{-1}\begin{bmatrix}0\\-1\end{bmatrix}. \tag{18}$$

Note that $\tilde{u}_z(x,\omega)$ in Eq. (15) is only defined in the range $(0\leqslant x\leqslant L)$. However, since it is a periodic function of the second kind, it can be written as a function for all values of x using Fourier series representation as shown in Appendix A. This is done by substituting $\tilde{u}_z(x,\omega)$ from Eq. (15) in Eq. (33) of Appendix A to calculate $c_n(\omega)$. The expression of $c_n(\omega)$ is then substituted in Eq. (32) of Appendix A to get the following expression of $\tilde{u}_z(x,\omega)$ which is valid for all values of x

$$\begin{aligned}\tilde{u}_z(x,\omega)=&\sum_{n=-\infty}^{\infty}\sum_{p=1}^{8}\mathrm{i}a_p\tilde{Z}_p\left[\frac{\mathrm{e}^{-\mathrm{i}(\xi_n-\phi_p+\varpi/v-\omega/v)L}-1}{(\xi_n-\phi_p+\varpi/v-\omega/v)L}\right]\mathrm{e}^{\mathrm{i}(\xi_n+\varpi/v-\omega/v)x}+\tilde{U}\mathrm{e}^{\mathrm{i}((\varpi/v)-(\omega/v))x}\\&+\sum_{n=-\infty}^{\infty}\tilde{V}_n b_n\mathrm{e}^{\mathrm{i}(\xi_n+(\varpi/v)-(\omega/v))x}.\end{aligned} \tag{19}$$

Considering only a limited number of terms ($-n_{\max} \leqslant n \leqslant n_{\max}$), the previous equation has $2n_{\max}+9$ unknown; $(b_{-n_{\max}}, b_{-n_{\max}+1}, \ldots, b_0, \ldots, b_{n_{\max}-1}, b_{n_{\max}})$ and $(a_1, a_2, \ldots, a_8)$.

Substituting $\tilde{z}_2$, $\tilde{z}_3$, $\tilde{R}$ from Eqs. (19), (13) and (11), respectively, into Eq. (8) and extracting results of the same harmonic gives

$$\sum_{p=1}^{8} \mathrm{i}a_p \tilde{Z}_p(2,1)\left[\frac{\mathrm{e}^{-\mathrm{i}(\xi_n-\phi_p+\varpi/v-\omega/v)L}-1}{(\xi_n-\phi_p+\varpi/v-\omega/v)L}\right] + \tilde{U}(2,1) + b_n\left[\tilde{V}_n(2,1) - \tilde{H}_t\left(\xi_n+\frac{\varpi}{v}-\frac{\omega}{v},\omega\right)+1/k_2\right] = 0$$

for $n = 0$, (20.1)

$$\sum_{p=1}^{8} \mathrm{i}a_p \tilde{Z}_p(2,1)\left[\frac{\mathrm{e}^{-\mathrm{i}(\xi_n-\phi_p+\varpi/v-\omega/v)L}-1}{(\xi_n-\phi_p+\varpi/v-\omega/v)L}\right] + b_n\left[\tilde{V}_n(2,1) - \tilde{H}_t\left(\xi_n+\frac{\varpi}{v}-\frac{\omega}{v},\omega\right)+1/k_2\right] = 0$$

for all other values of n. (20.2)

Eqs. (20.1) and (20.2) along with the eight boundary conditions represent the necessary $2n_{\max}+9$ equations to calculate all the unknowns b_n and a_p. Using these values, Eq. (13) is employed to calculate the response at any position in the soil by using the suitable FRF from the PiP model as discussed before. The displacements in the space-frequency domain are transformed to the space-time domain numerically using the discrete Fourier transform.

3. Results and discussion

In this section, calculations of the model presented in the previous section are demonstrated by an example of a floating-slab track with discontinuous slabs of length $L = 6\,\mathrm{m}$. The track is subjected to a harmonic force moving with a constant velocity $v = 40\,\mathrm{km/h}$. The track consists of two rails of type UIC60 with bending stiffness $EI_1 = 12.9\,\mathrm{MPa\,m^4}$ and mass per unit length $m_1 = 120.6\,\mathrm{kg/m}$. The track's concrete-slab has a bending stiffness $EI_2 = 1430\,\mathrm{MPa\,m^4}$ and mass per unit length $m_2 = 3500\,\mathrm{kg/m}$. The stiffness of the railpads and slab bearings per unit length are $k_1 = 200\,\mathrm{MN/m/m}$ (with hysteretic loss factor of $\eta_{k1} = 0.3$) and $k_2 = 5\,\mathrm{MN/m/m}$ (with hysteretic loss factor of $\eta_{k2} = 0.5$), respectively. The tunnel is made of concrete with compression wave velocity $c_1 = 5189\,\mathrm{m/s}$, shear wave velocity $c_2 = 2774\,\mathrm{m/s}$, density $\rho = 2500\,\mathrm{kg/m^3}$ (with hysteretic loss factor of $\eta = 0.015$ associated with both pressure and shear wave velocities). The tunnel has external radius $r_2 = 3.0\,\mathrm{m}$ and internal radius $r_1 = 2.75\,\mathrm{m}$. The soil parameters are those for Oxford Clay and Middle Chalk with compression wave velocity $c_1 = 944\,\mathrm{m/s}$, shear wave velocity $c_2 = 309\,\mathrm{m/s}$ and density $\rho = 2000\,\mathrm{kg/m^3}$ (with hysteretic loss factor of $\eta = 0.03$ associated with both pressure and shear wave velocities). The distance between the tunnel centre and the free surface is 20 m. It is found that for the given parameters in this section, a value of $n_{\max} = 10$ gives converged results for excitation frequencies below 200 Hz.

Fig. 2a and b shows the displacements in the frequency domain at a point in the free-surface at ($x = 0\,\mathrm{m}$, $y = 10\,\mathrm{m}$, $z = 0\,\mathrm{m}$, see Fig. 1 for information about the coordinate systems) for a moving unit-force with excitation frequencies: (a) $\bar{f} = 30\,\mathrm{Hz}$; and (b) $\bar{f} = 80\,\mathrm{Hz}$. These results are presented to demonstrate the response in the frequency domain and the two excitation frequencies are selected only as examples. It can be seen from these figures that displacements are large at and near a frequency equal to the excitation frequency. The displacement away from this frequency attenuates quickly. This is an important remark when performing the Discrete Fourier transformation because frequencies with insignificant values of displacements can be excluded from the numerical integration. The results in the frequency domain presented in this section are calculated in the range $[\bar{f}-10, \bar{f}+10]\,\mathrm{Hz}$ (where $\bar{f}$ is the excitation frequency) with a step $\Delta f = 0.05\,\mathrm{Hz}$. The selected frequency-range and interval are found to give converged results in the time domain for the given parameters of the track, tunnel and soil. The displacements' curves in Fig. 2 also show undulation with a constant step of 1.85 Hz between pronounced troughs. This step results from the moving load on the periodic track and can be calculated by $f_s = v/L$.

Fig. 3a and b shows the displacements in the time domain in the free-surface at ($x = 0\,\mathrm{m}$, $y = 10\,\mathrm{m}$, $z = 0\,\mathrm{m}$) for a unit force moving on the track with two excitation frequencies: (a) $\bar{f} = 30\,\mathrm{Hz}$; and (b) $\bar{f} = 80\,\mathrm{Hz}$. These

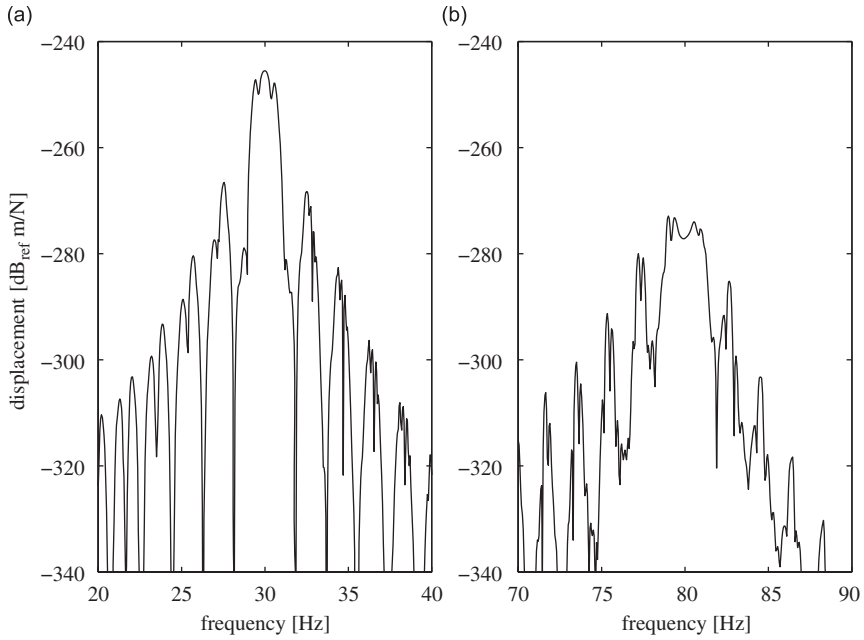

Fig. 2. The displacements in the frequency domain at $x = 0$ m, $y = 10$ m, $z = 0$ m due to a harmonic load with excitation frequency: (a) 30 Hz and (b) 80 Hz. The load is moving with a constant velocity 40 km/h.

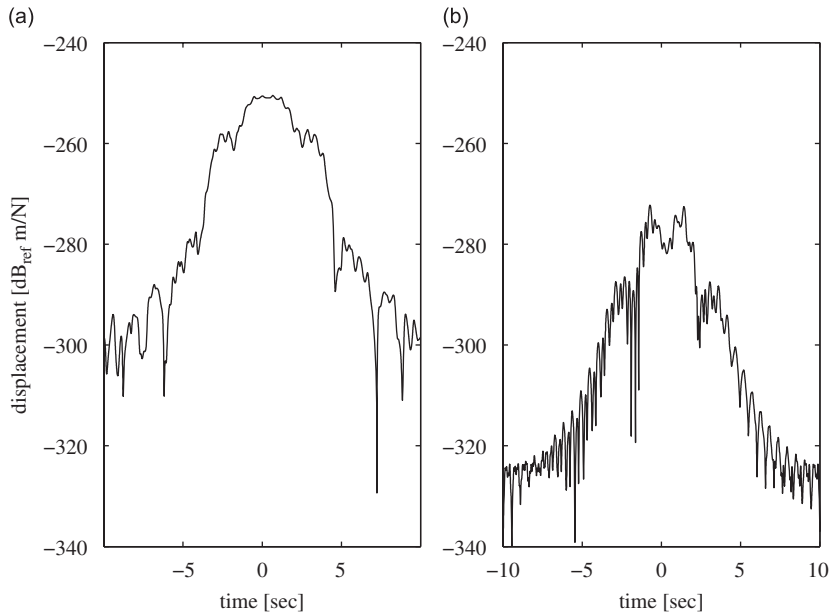

Fig. 3. The displacements in the time domain at $x = 0$ m, $y = 10$ m, $z = 0$ m due to a harmonic load with excitation frequency: (a) 30 Hz and (b) 80 Hz. The load is moving with a constant velocity 40 km/h.

results are calculated by transforming the results in Fig. 2a and b using the discrete Fourier transformation. According to Nyquist criterion, the range of time for a frequency step of $\Delta f = 0.05$ Hz is $(-10 \leqslant t \leqslant 10)$ s. This covers a distance in the range $(-111 \leqslant x \leqslant 111)$ m for the moving load with a velocity 40 km/h. It can be seen

from Fig. 3a and b that the maximum displacement at a point in the soil occur at different times when comparing the displacements due to different excitation frequencies.

The next results compare the maximum displacements in the free surface for a harmonic moving load on a track with discontinuous slab to those produced by a track with a continuous slab. The latter results are calculated using a continuous model of a track-tunnel-soil formulated in the wavenumber-frequency domain and results are then transformed to the space-time domain [7–9].

Fig. 4 shows the maximum displacements at a point in the free surface at ($x = 0$ m, $y = 10$ m, $z = 0$ m) for excitations frequencies in the range 1–200 Hz. At each excitation frequency, displacements are calculated in the frequency domain as exemplified by Fig. 2a and b. Results are then transformed to the time domain as exemplified by Fig. 3a and b and the maximum displacement at each excitation frequency is recorded. The process is then repeated for all excitation frequencies in the frequency range of interest to produce the results in Fig. 4. Note that both curves have peaks at 6 Hz, this corresponds to the resonance frequency of the slab on the slab bearings which can be calculated by $(1/2\pi)\sqrt{k_2/m_2}$.

It can be seen from Fig. 4 that the displacements for the track with the discontinuous slab have two pronounced peaks at 63 and 174 Hz. At these frequencies, displacements at the free-surface from the track with the discontinuous slab can exceed those resulting from the track with the continuous slab by more than 10 dB. The peaks are attributed to standing waves which are built by reflections of propagating waves at free ends of the slab. The frequencies of these peaks can be calculated from the free–free beam natural frequencies, see Ref. [23] for example, which reads

$$f_n = \sqrt{\frac{EI_2}{m_2}}\frac{\lambda_n^2}{2\pi L^2}, \tag{21}$$

where $\lambda_1 = 4.73$, $\lambda_2 = 7.853$, $\lambda_3 = 10.996$, etc.

For the current parameters of the track, the first two natural frequencies occur at about 63 and 174 Hz, which agree with the results in Fig. 4.

Fig. 5a and b shows snap shots for the displacements of the discrete slab at time $t = 0.5\,L/v$ for harmonic loads with excitation frequencies 63 and 174 Hz, respectively. These figures confirm again that at 63 Hz, the slab is resonating with the first free–free bending mode and at 174 Hz, the slab is resonating with the second free–free bending mode.

Fig. 6 shows the maximum displacements at a different point in the free surface at ($x = 0$ m, $y = 20$ m, $z = 0$ m) for excitations frequencies in the range 1–200 Hz. Again, the displacement of a track with discontinuous slab show pronounced peaks at the resonance frequencies of the slab.

The study presented in this paper has drawn the attention to the unfavourable vibration increase resulting from floating-slab tracks with discontinuous slabs. In reality, more resonances are expected due to bending

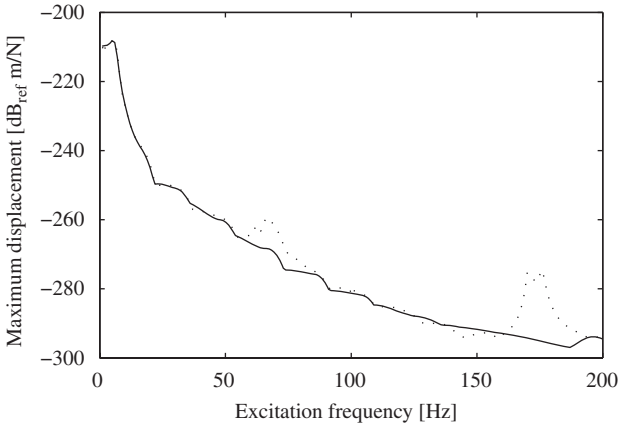

Fig. 4. The maximum displacement at $x = 0$ m, $y = 10$ m, $z = 0$ m due to a harmonic load moving with a constant velocity 40 km/h on (-) a track with continuous slab and (- -) a track with a discontinuous slab.

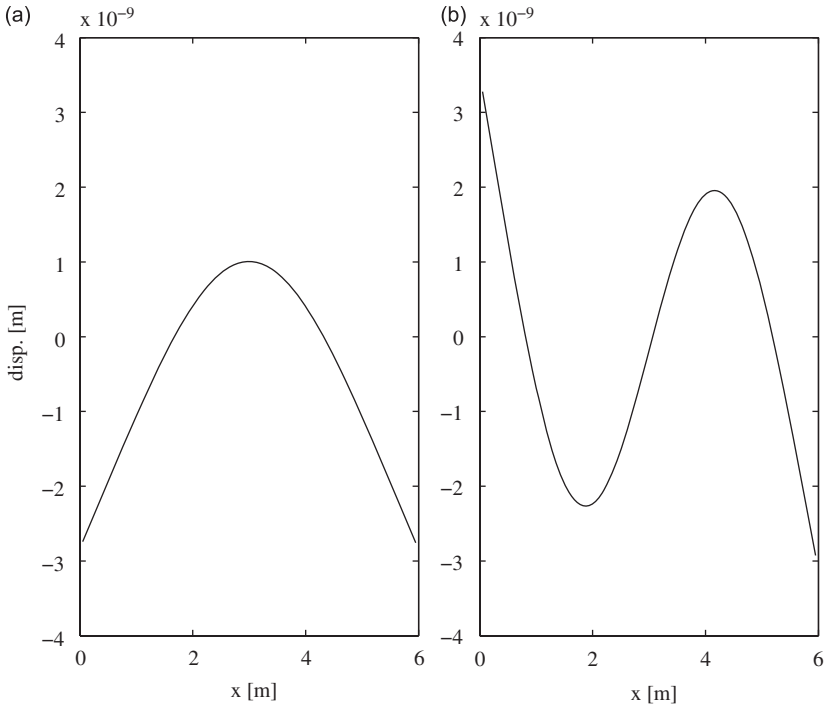

Fig. 5. A snap shot of the slab at $t = L/v = 0.54$ s for a moving load on the track with a harmonic excitation: (a) 63 Hz and (b) 174 Hz.

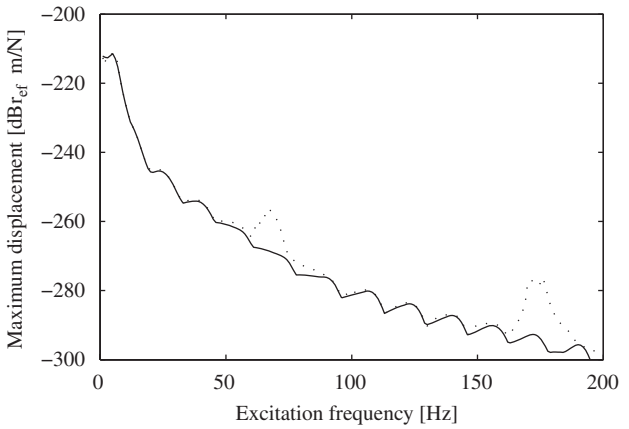

Fig. 6. The maximum displacement at $x = 0$ m, $y = 20$ m, $z = 0$ m due to a harmonic load moving with a constant velocity 40 km/h on (-) a track with continuous slab and (- -) a track with a discontinuous slab.

resonances across the width of the slab. Moreover, other modes of slab, e.g. the torsion mode, can be excited if the forces on the two rails are not equal or have some phase difference.

The current model has only addressed the case of a harmonic moving load on floating tracks with discontinuous slabs. To understand the dynamics of a train running on such a track and the effect on vibration in the far field, a model of a train should be coupled to the track. This model is currently under development by the authors.

4. Conclusions

A new model for calculating vibration from floating-slab tracks with discontinuous slabs in underground railway tunnels is presented. The model employs the periodic-infinite structure theory to couple a periodic track to a continuous model of a tunnel embedded in a half-space where calculations are performed in the space-frequency domain. The frequency response functions of the tunnel-soil system are calculated using a new version of the PiP model which is presented in a different paper. The displacements at the free-surface are calculated and compared with those of tracks with continuous slabs. A floating-slab track with a discontinuous slab results into more vibration at the resonance frequencies of the slab. These frequencies can be calculated using the equation of the natural frequencies of a free–free beam.

Appendix A

A.1. The periodic-infinite structure theory

The purpose of this appendix is to provide a quick derivation of the main relationships governing the behaviour of a periodic-infinite structure when subjected to a harmonic moving load.

The first relationship is the periodicity condition. For a periodic structure with periodicity L in the x direction subjected to a point force moving with a constant velocity v, the displacement at time t for a point at distance x is given by the following convolution integral

$$u(x,t)=\int_{-\infty}^{\infty}F(\tau)h(x,\tau v,t-\tau)\,\mathrm{d}\tau, \tag{22}$$

where $F(\tau)$ is the value of the force at time $t=\tau$, $h(x_1,x_2,t_1)$ is the impulse response function which expresses the displacement at $x=x_1$ and time $t=t_1$ due to a unit impulse applied at $x=x_1$ and time $t=0$. Note that due to periodicity, the following relationship holds

$$h(x_1+L,x_2+L,t_1)=h(x_1,x_2,t_1). \tag{23}$$

Form Eq. (22), the displacement at time $t+L/v$ for a point at distance $x+L$ is given by

$$u(x+L,t+L/v)=\int_{-\infty}^{\infty}F(\tau)h(x+L,\tau v,t+L/v-\tau)\,\mathrm{d}\tau. \tag{24}$$

The last equation can be written as

$$u(x+L,t+L/v)=\int_{-\infty}^{\infty}F(\tau+L/v)h(x+L,\tau v+L,t-\tau)\,\mathrm{d}\tau. \tag{25}$$

Substituting $h(x+L,\ \tau v+L,\ t-\tau)=h(x,\ \tau v,\ t-\tau)$ and for a harmonic moving load $F(\tau+L/v)=F(\tau)\mathrm{e}^{\mathrm{i}\omega L/v}$ results in

$$u(x+L,t+L/v)=\mathrm{e}^{\mathrm{i}\varpi L/v}u(x,t), \tag{26}$$

which is known as the periodicity condition. The function u in the previous equation is periodic in both space and time. The periodicity is reserved to only one variable by transforming the equation to the space-frequency domain, which results in

$$\tilde{u}(x+L,\omega)=\mathrm{e}^{\mathrm{i}(\varpi-\omega/v)L}\tilde{u}(x,\omega). \tag{27}$$

Eq. (27) shows that $\tilde{u}$ is a periodic function of the second kind which can be transformed into an equation with periodicity of the first kind using the following substitution

$$\tilde{g}(x,\omega)=\mathrm{e}^{-\mathrm{i}(\varpi-\omega/v)x}\tilde{u}(x,\omega). \tag{28}$$

From Eqs. (28) and (27), one can write

$$\tilde{g}(x+L,\omega)=\tilde{g}(x,\omega). \tag{29}$$

Eq. (29) shows that $\tilde{g}$ is a periodic function of the first kind. This equation can be written as a summation of Fourier series as, see Ref. [24] for example

$$\tilde{g}(x,\omega)=\sum_{n=-\infty}^{\infty}c_n(\omega)\mathrm{e}^{\mathrm{i}\xi_n x}\quad\text{with }\xi_n=\frac{2\pi n}{L}. \tag{30}$$

The value of $c_n(\omega)$ can be calculated from the following relationship

$$c_n(\omega)=\frac{1}{L}\int_0^L\tilde{g}(x,\omega)\mathrm{e}^{-\mathrm{i}\xi_n x}\mathrm{d}x. \tag{31}$$

Using Eqs. (28), (30) and (31), the value of $\tilde{u}(x,\omega)$ and the coefficients $c_n(\omega)$ can be calculated from

$$\tilde{u}(x,\omega)=\sum_{n=-\infty}^{\infty}c_n(\omega)\mathrm{e}^{\mathrm{i}(\xi_n+(\varpi/v)-(\omega/v))x}\quad\text{with }\xi_n=\frac{2\pi n}{L}, \tag{32}$$

$$c_n(\omega)=\frac{1}{L}\int_0^L\tilde{u}(x,\omega)\mathrm{e}^{-\mathrm{i}(\xi_n+(\varpi/v)-(\omega/v))x}\,\mathrm{d}x. \tag{33}$$

References

[1] G.P. Wilson, H.J. Saurenman, J.T. Nelson, Control of ground-borne noise and vibration, *Journal of Sound and Vibration* 87 (2) (1981) 339–350.

[2] J.T. Nelson, Recent developments in ground-borne noise and vibration control, *Journal of Sound and Vibration* 193 (1) (1996) 367–376.

[3] H. Saurenman, J. Philips, In-service tests of the effectiveness of vibration control measures on the BART rail transit system, *Journal of Sound and Vibration* 293 (3–5) (2006) 888–900.

[4] M. Shamalta, A.V. Metrikine, Analytical modelling of the dynamic response of an embedded railway track to a moving load, *Archive of Applied Mechanics* 73 (1–2) (2003) 131–146.

[5] M.F.M. Hussein, H.E.M. Hunt, Modelling of floating-slab tracks with continuous slabs under oscillating-moving loads, *Journal of Sound and Vibration* 297 (1–2) (2006) 37–54.

[6] G. Lombaert, G. Degrande, B. Vanhauwere, B. Vandeborght, S. François, The control of ground-borne vibrations from railway traffic by means of continuous floating slabs, *Journal of Sound and Vibration* 297 (3–5) (2006) 946–961.

[7] J.A. Forrest, H.E.M. Hunt, A three-dimensional model for calculation of train-induced ground vibration, *Journal of Sound and Vibration* 294 (4–5) (2006) 678–705.

[8] J.A. Forrest, H.E.M. Hunt, Ground vibration generated by trains in underground tunnels, *Journal of Sound and Vibration* 294 (4–5) (2006) 706–736.

[9] M.F.M. Hussein, H.E.M. Hunt, A numerical model for calculating vibration from a railway tunnel embedded in a full-space, *Journal of Sound and Vibration* 305 (3) (2007) 401–431.

[10] M.F.M. Hussein, H.E.M. Hunt, Modelling of floating-slab track with discontinuous slab, part I: response to oscillating moving loads, *Journal of Low Frequency Noise, Vibration and Active Control* 25 (1) (2006) 23–40.

[11] M.F.M. Hussein, H.E.M. Hunt, Modelling of floating-slab track with discontinuous slab, part 2: response to moving trains, *Journal of Low Frequency Noise, Vibration and Active Control* 25 (2) (2006) 111–118.

[12] M.F.M. Hussein, S. Gupta, H.E.M. Hunt, G. Degrande, J.P. Talbot, An efficient model for calculating vibration from a railway tunnel buried in a half-space, *Proceeding of the 13th International Congress on Sound and Vibration* (*ICSV13*), Vienna, Austria, 2–6 July 2006.

[13] L. Jezequel, Response of periodic systems to a moving load, *Journal of Applied Mechanics, Transaction of the ASME* 48 (3) (1981) 613–618.

[14] J. Kisilowski, Z. Strzyzakowski, B. Sowinski, Application of discrete-continuous model systems in investigating dynamics of wheelset-track system vertical vibration, *Zeitschrift fü*r Angewandte Mathematik und Mechanik 68 (94) (1988) 70–71.

[15] H. Ilias, S. Muller, A discrete-continuous track-model for wheelsets rolling over short wavelength sinusoidal rail irregularities, *Vehicle System Dynamics* 23 (Suppl.) (1994) 221–233.

[16] T. Krzyzynski, On continuous subsystem modelling in the dynamic interaction problem of a train-track-system, *Vehicle System Dynamics* 24 (Suppl.) (1995) 311–324.

[17] S. Muller, T. Krzyzynski, H. Ilias, Comparison of semi-analytical methods of analysing periodic structures under a moving load, *Vehicle System Dynamics* 24 (Suppl.) (1995) 325–339.

[18] A. Nordborg, Vertical rail vibration: point force excitation, *Acta Acoustica* 84 (2) (1998) 280–288.

[19] A. Nordborg, Vertical rail vibration: parametric excitation, *Acta Acoustica* 84 (2) (1998) 289–300.

[20] C.C. Smith, D.N. Wormley, Response of continuous periodically supported guideway beams to travelling vehicle loads, *Journal of Dynamic Systems, Measurements and Control, Transaction of the ASME* 97 (1975) 21–29.
[21] P.M. Belotserkovskiy, Forced oscillations of infinite periodic structures. Applications to railway track dynamics, *Vehicle System Dynamics* 28 (Suppl.) (1998) 85–103.
[22] A.V. Metrikine, A.L. Bosch, Dynamic response of a two-level catenary to a moving load, *Journal of Sound and Vibration* 292 (3–5) (2006) 676–693.
[23] R.D. Blevins, *Formulas for Natural Frequency and Mode Shape*, fourth ed., Krieger Publishing Company, Florida.
[24] K.F. Riley, M.P. Hobson, S.J. Bence, *Mathematical Methods for Physics and Engineering*, Cambridge University Press, Cambridge, 2000.